ADVANCED FUNCTIONAL MATERIALS
www.afm-journal.de

Hyperbranched Polyglycerol-Grafted Superparamagnetic Iron Oxide Nanoparticles: Synthesis, Characterization, Functionalization, Size Separation, Magnetic Properties, and Biological Applications

*Li Zhao, Tokuhiro Chano, Shigehiro Morikawa, Yukie Saito, Akihiko Shiino, Sawako Shimizu, Takuro Maeda, Takayoshi Irie, Shuji Aonuma, Hidetoshi Okabe, Takahide Kimura, Toshiro Inubushi, and Naoki Komatsu**

For biomedical application of nanoparticles, the surface chemical functionality is very important to impart additional functions, such as solubility and stability in a physiological environment, and targeting specificity as an imaging probe and a drug carrier. Although polyethylene glycol (PEG) has been used extensively, here, it is proposed that hyperbranched polyglycerol (PG) is a good or even better alternative to PEG. Superparamagnetic iron oxide nanoparticles (SPIONs) prepared using a polyol method are directly functionalized with PG through ring-opening polymerization of glycidol. The resulting SPION-PG is highly soluble in pure water (>40 mg mL^{-1}) and in a phosphate buffer solution (>25 mg mL^{-1}). Such high solubility enables separation of SPION-PG according to size using size exclusion chromatography (SEC). The size-separated SPION-PG shows a gradual increase in transverse relaxivity (r_2) with increasing particle size. For biological application, SPION-PG is functionalized through multistep organic transformations (–OH → –OTs (tosylate) → –N_3 → –RGD) including click chemistry as a key step to impart targeting specificity by immobilization of cyclic RGD peptide (Arg-Gly-Asp-D-Tyr-Lys) on the surface. The targeting effect is demonstrated by the cell experiments; SPION-PG-RGD is taken up by the cells overexpressing $\alpha_v\beta_3$-integrin such as U87MG and A549.

1. Introduction

Good solubility of individualized nanoparticles in a physiological environment is vital for their biomedical application as an imaging probe and a drug carrier. In this context, extensive investigations have been carried out for preparation of individualized nanoparticles with high solubility. Polyethylene glycol (PEG) is most frequently used as dispersant due to their hydrophilicity together with biocompatible and anti-biofouling properties.[1–3] In our experience of nanodiamond (ND), however, the aqueous solubility of PEG-functionalized ND (ND-PEG) is not sufficient for their biomedical applications.[4] In order to impart better solubility to ND, we added the hydroxyl branches to the PEG chain in the molecular design and carried out polyglycerol (PG) grafting through ring-opening polymerization of glycidol initiating from the surface of ND.[5–7] As a result, PG-functionalized ND (ND-PG) exhibited 400 times larger solubility

Dr. L. Zhao, S. Shimizu, T. Maeda, T. Irie,
Prof. T. Kimura, Prof. N. Komatsu
Department of Chemistry
Shiga University of Medical Science
Seta, Otsu 520-2192, Japan
E-mail: nkomatsu@belle.shiga-med.ac.jp
Prof. T. Chano, S. Shimizu, Prof. H. Okabe
Department of Clinical Laboratory Medicine
Shiga University of Medical Science
Seta, Otsu 520-2192, Japan
Prof. S. Morikawa, Prof. A. Shiino, Prof. T. Inubushi
Biomedical MR Science Center
Shiga University of Medical Science
Seta, Otsu 520-2192, Japan
Prof. Y. Saito
Graduate School of Agricultural and Life Sciences
The University of Tokyo
1-1-1 Yayoi, Bunkyo-ku, Tokyo 113-8657, Japan
T. Irie, Prof. S. Aonuma
Department of Applied Chemistry
Osaka Electro-Communication University
Neyagawa, Osaka 572-8530, Japan

DOI: 10.1002/adfm.201201060

in phosphate buffer saline (PBS) than ND-PEG because of more hydrophilic nature of hydroxyl group than ether linkage and much denser coverage of the ND surface with hyperbranched PG than linear PEG.[8] We also found that the PG grafting is effective in preparing stable aqueous hydrosol of individualized nanoparticles, enabling us to separate the size of the ND-PG by size-exclusion chromatography (SEC). PG is reported to be as biocompatible as,[9] more resistant to protein adsorption than,[10] and more amenable for further chemical derivatization than PEG. PG can be concluded as better alternative to PEG in view of biomedical applications. In addition, the PG functionalization is found to be applied to not only ND, but also inorganic nanoparticle such as zinc oxide to prepare stable hydrosol with good solubility in a physiological environment.[11] We expect that this methodology can be applied to a wide variety of nanomaterials to provide them with sufficient properties for their biomedical applications, such as aqueous solubility and stability in a solution, biocompatibility, and protein-resistivity. In particular, this methodology is promising to give general solution towards the common problem of nanoparticle agglomeration in a solution, which is an intrinsic property of most nanoparticles.[12]

Superparamagnetic iron oxide nanoparticles (SPIONs) are one of the most well-known nanoparticles used in biomedical applications, especially as a magnetic resonance imaging (MRI) probe for diagnosis, and as a drug carrier and a hyperthermic agent for therapy.[13–20] These applications frequently require good solubility and high stability of the nanoparticle in a physiological environment, and strict control of the size and the surface chemical functionality.[21,22] In order to fulfill these requirements, SPION has been wrapped with dispersant polymers.[13,23] Most of the commercial SPIONs are coated with dextran and its derivatives.[17] Although dextran-coating imparts good aqueous solubility to SPION, this results in increase of the particle size and broadening of the size distribution compared to the size and size distribution of the individual SPION. In order to prepare a stable aqueous solution and regulate the size of SPION, ligands with high affinity to the surface of SPION have been investigated to immobilize hydrophilic polymers such as PEG on the surface.[7,13,23,24] On the other hand, SPION prepared via polyol process was reported to have intrinsic hydrophilicity due to the hydroxyl groups on the surface.[25,26] This is in marked contrast to SPION prepared by conventional coprecipitation[27] and high-temperature decomposition in organic phase,[17,28] which is hydrophobic.[19,26,29] Quite recently, the hydroxyl groups on the hydrophilic SPION were proven to serve as the starting functionality for multistep covalent transformations on the surface.[30] This implies that we do not need anchoring ligands to immobilize hydrophilic polymers on the surface of SPION and that we can utilize the hydroxyl groups on the surface to graft hydrophilic polymers directly.[7] Herein, we report on the direct PG functionalization on the surface of SPION to impart high solubility in a physiological medium and further covalent chemical functionalization to add a targeting property for cancer cell. We also realized chromatographic size separation of the PG-functionalized SPION (SPION-PG)[1,8,31] and confirmed the relationship between the particle size and the magnetic properties.[1,32–34]

2. Results and Discussion

2.1. Synthesis and Characterization of SPION

SPION was synthesized by thermal decomposition of iron (III) acetylacetonate in triethylene glycol (TREG) at high temperature according to the reported procedure.[25,26] Powder X-ray diffraction (XRD) reveals that the prepared sample is Fe_3O_4 (magnetite) with a highly crystalline inverse spinel structure (Supporting Information Figure S1). From the scanning transmission electron microscopy (STEM) image shown in **Figure 1**a, the prepared SPION is found to be spherical with average diameter of 8.8 ± 2.2 nm. The highly crystalline structure of the as-prepared SPION is also confirmed by high-resolution transmission electron microscopy (HRTEM); (311) crystallographic layers are clearly observed in Figure 1b. However, the results of elemental analysis (**Table 1**) and IR spectrum (**Figure 2**a) indicate that small portion of organic component is included in the nanoparticles. C and H were detected in the elemental analysis, and absorption of O–H and C–H was observed in the IR spectrum. Taking into account these results as well as the reaction conditions to prepare the SPION, the organic contaminant in the as-prepared one should be TREG and/or its derivatives.[25,26,30] In fact, the C:H ratio of the organic contaminant (78:22) calculated from the result of the elemental analysis (Table 1) is not so different from that of TREG (84:16) calculated from the molecular formula and weight.

The ratio between the TREG and SPION can be estimated by the results of elemental analysis and thermogravimetric analysis (TGA) shown in Table 1 and **Figure 3**, respectively. If the weight (95.10 wt%) other than C and H in the elemental analysis of SPION is occupied by Fe from Fe_3O_4, and O from TREG (molecular formula: $C_6H_{14}O_4$) and Fe_3O_4, wt% of Fe and O is calculated to be 66.37% and 28.73%, respectively. This weight ratio of C (3.80%):Fe (66.37%):O (28.73%) is corresponding to the following ratio in number of these atoms; C (6):Fe (22):O (34), indicating that the ratio of TREG:Fe_3O_4 is calculated to be about 1:7.4 in number and 1:11 in weight. Since the Fe_3O_4 core consists of highly crystalline structure as mentioned above, most of TREG molecules are considered to be adsorbed on and/or included near the surface of the SPION. The weight reduction (8.9% at 450 °C) in TGA shown in Figure 3a is consistent with the weight% of TREG (8%) calculated from the above weight ratio (TREG:Fe_3O_4 = 1:11), supporting the existence of TREG near surface region. Some TREGs are considered to be just physisorbed on the surface of the iron oxide nanoparticle through van der Waals interaction as reported by Santamaria et al.[30] However, coordination bonding between iron in Fe_3O_4 and oxygen in TREG is also conceivable as reported by Maity et al.,[35] sustaining TREG or its derivatives on the surface of SPION more tightly. In fact, the weight of the as-prepared SPION was continued to decrease in TGA (Figure 3a) even after the temperature exceeded the boiling point of TREG (285 °C). In addition, iron is hard Lewis acid to bear strong affinity toward hard Lewis base such as oxygen. Therefore, we can conclude that a significant number of hydroxyl groups are supposed to stably exist in the surface region of the SPION and that the hydroxyl groups, bearing increased nucleophilicity through coordination bonding with iron,[35] may initiate PG grafting

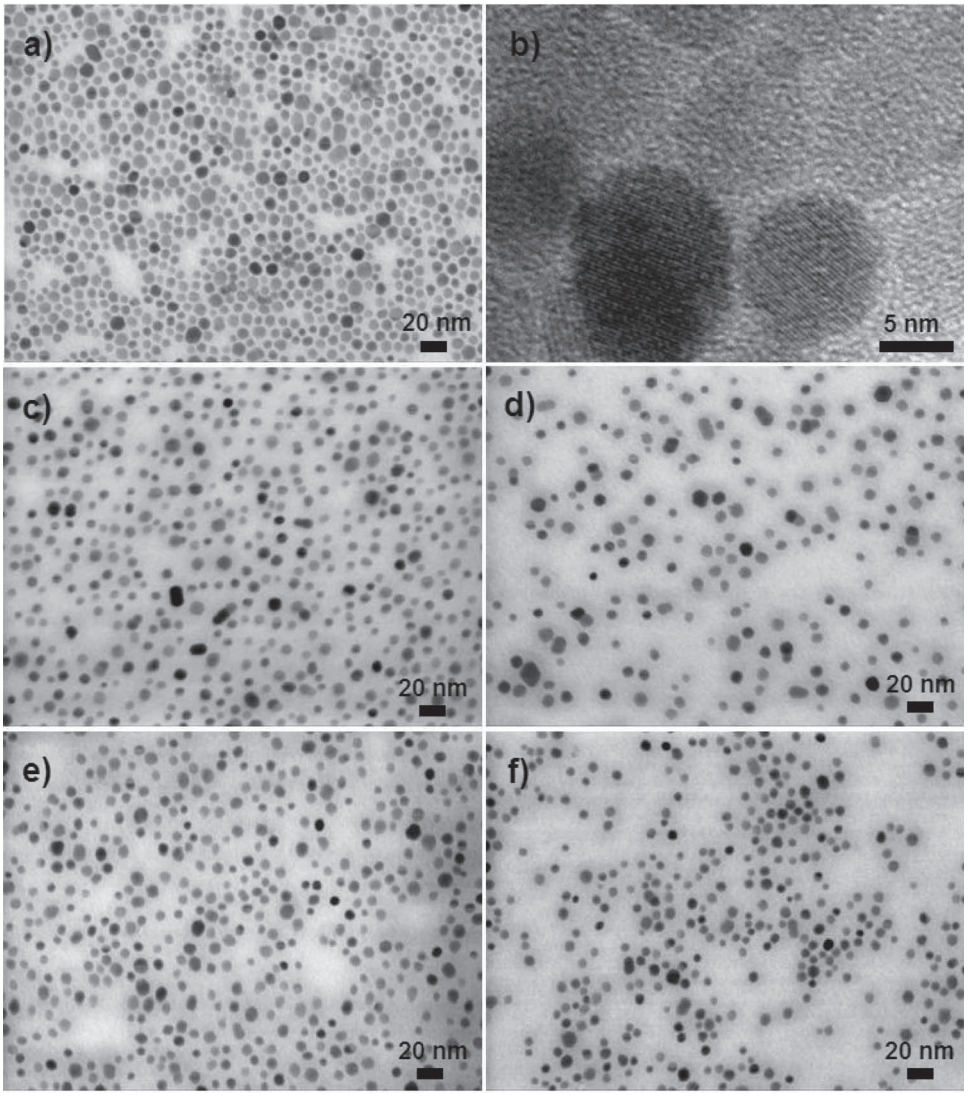

Figure 1. a) STEM and b) HRTEM images of as-synthesized SPION and STEM images of SPION-PG c) before chromatographic separation, d) fraction 1, e) fraction 2, and f) fraction 3 after chromatographic separation.

Table 1. Elemental analyses of as-prepared and functionalized SPIONs.

	C [wt%]	H [wt%]	N [wt%]
SPION	3.80	1.10	0.00
SPION-PG	30.60	5.83	0.00
SPION-PG-N_3	24.51	4.90	1.11

through ring-opening polymerization of glycidol on the surface of SPION, as will be mentioned below.[8]

2.2. PG-Functionalization of SPION and Characterization of SPION-PG

In order to increase the solubility of SPION sufficient for biomedical application, we intended to initiate the ring-opening polymerization of glycidol at the hydroxyl groups on the surface of SPION as shown in **Scheme 1**. Under the same reaction conditions as those in our previous papers,[8,11] we bath-sonicated and, then, heated the suspension of SPION in glycidol without any additives such as acid and base. The SPION was well dispersed in glycidol with the aid of bath sonication owing to the hydroxyl groups on the surface, discussed above. After washing and lyophilizing, blackish flocculent solid (52.3 mg) was obtained from the starting SPION (30 mg).

The obtained solid was characterized qualitatively by FTIR, STEM, and dynamic light scattering (DLS), and quantitatively by TGA and elemental analysis. Since the nanoparticle after the reaction, shown in STEM image (Figure 1c), has the same shape (sphere), average diameter, and standard deviation (SD) (8.8 ± 2.3 nm) as that (8.8 ± 2.2 nm) before the reaction (Figure 1a), we conclude that the core is individual SPION. The PG grafting, as shown in Scheme 1, was confirmed by large increase of the absorption bands at 3400, 2900, and 1100 cm^{-1} corresponding

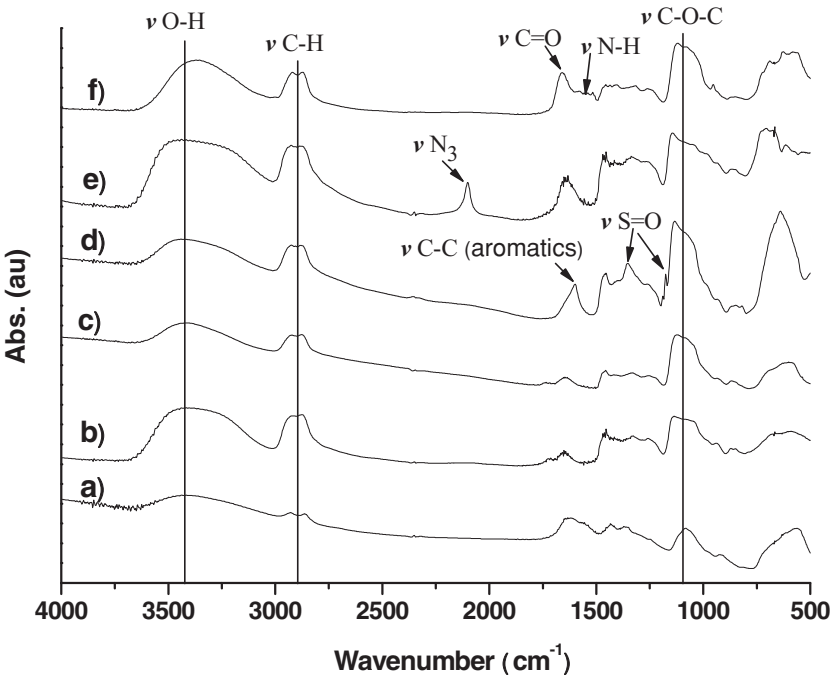

Figure 2. FTIR spectra of a) as-synthesized SPION, b) free PG, c) SPION-PG, d) SPION-PG-OTs, e) SPION-PG-N_3, and f) SPION-PG-RGD. Arrows indicate new absorption bands after each transformation.

to O–H, C–H, and C–O–C stretchings, respectively, as in the cases of ND- and ZnO-PG.[8,11] This is also supported by the fact that the FTIR spectrum of SPION-PG (Figure 2c) is similar to that of free PG (Figure 2b), which is prepared by ring-opening polymerization of glycidol in the absence of SPION but otherwise under the same conditions. The mean hydrodynamic diameter and the SD of the water-soluble SPION-PG was determined to be 24.9 ± 5.1 nm on the basis of the number distribution by DLS (Supporting Information Figure S2 and **Table 2**). The difference between the hydrodynamic diameter of SPION-PG by DLS (Supporting Information Figure S2b) and the core one by STEM image (Figure 1c) is considered to correspond to the thickness of the PG layer on the iron oxide core. The thickness of PG of the SPION-PG in water, calculated to be 8.9 nm (Table 2), is similar to that of ND-PG (11 nm).[8] Similar thickness of the PG coatings on smaller core of SPION (8.8 nm) than ND (30 nm) may realize much higher aqueous solubility of the SPION-PG (>40 mg mL^{-1}) than ND-PG (>20 mg mL^{-1}), as will be discussed below (**Figure 4**).

From the result of the elemental analysis of SPION-PG shown in Table 1, we can also estimate the weight ratio between the inner core of SPION and the outer shell consisting of TREG and PG. The weight of one spherical Fe_3O_4 nanoparticle with average diameter of 8.8 nm is 1.8 ag, which is calculated from the volume of the nanoparticle (357 nm^3) and the density of magnetite (5.1 g cm^{-3}). The weight of TREG in and/or on the nanoparticle is caluculated to be 0.17 ag from the weight ratio between SPION and TREG (11:1), discussed above. Since the weight (%) other than C, H, and N in the elemental analysis, 63.57%, corresponds to the weight (%) of Fe and O, the weight ratio of C:(Fe + O) is 30.60:63.57 in Table 1. C, Fe, and O in SPION-PG consist of $C_{TREG} + C_{PG}$, Fe_{SPION}, and $O_{SPION} + O_{TREG} + O_{PG}$, respectively, where C_{TREG}, C_{PG}, Fe_{SPION}, O_{SPION}, O_{TREG}, and O_{PG} denote C in TREG and PG, Fe in SPION, and O in SPION, TREG, and PG, respectively. From the weight ratio of $(C_{TREG} + C_{PG})$:$(Fe_{SPION} + O_{SPION} + O_{TREG} + O_{PG})$ = 30.60:63.57, the weight of the PG layer in one particle is calculated to be 2.9 ag (see the Supporting Information). Based on the above calculations, the weight of one SPION-PG with the average size is determined to be 4.9 ag and the weight ratio of SPION core (1.8 ag):PG (2.9 ag):TREG (0.17 ag) is 37:60:3.

The ratio of the inner core and the outer shell (37:63) based on the result of the elemental analysis is slightly different from that determined by TGA (46:54) shown in Figure 3b. This is probably because a part of the organic component in the outer shell was converted to the carbon materials such as graphite and amorphous carbon at high temperature under a nitrogen atmosphere in TGA to increase the weight of nonvolatile component consisting mainly of SPION. In fact, about 5 weight% remained at high temperature in the TGA of free PG under

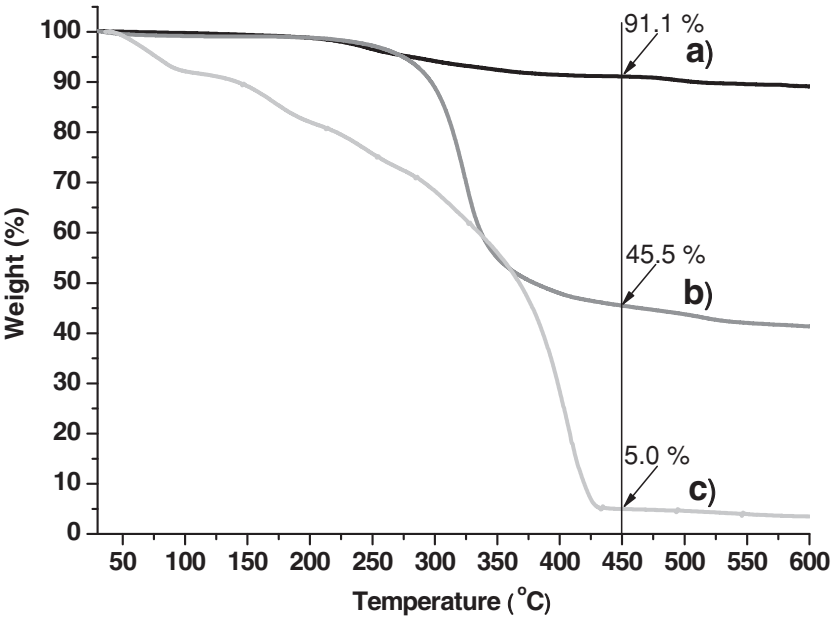

Figure 3. TGA profiles of a) as-synthesized SPION, b) SPION-PG, and c) free PG under N_2 atmosphere.

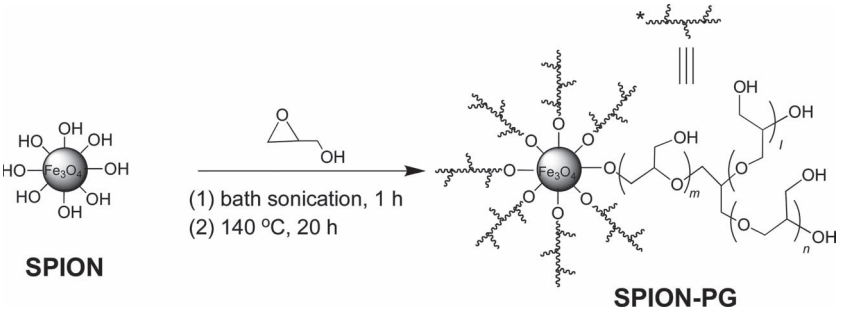

Scheme 1. Synthesis of SPION-PG through ring-opening polymerization of glycidol.

nitrogen as shown in Figure 3c, while free PG was fully combusted below 600 °C under air.[8]

The number of TREG and glycerol incorporated in one SPION-PG can be estimated from the amounts of TREG (0.17 ag) and PG (2.9 ag); 6.6×10^2 molecules of TREG and 2.4×10^4 units of glycerol are considered to consist of the outer shell. A degree of polymerization in SPION-PG is compared with that of ND-PG in **Table 3**.[8] In the number of glycidol grafted on the surface of the core, ND with average diameter of 30 nm is about 13 times larger than SPION with average diameter of 8.8 nm. When the number is divided by the surface area, SPION and ND exhibit similar values as shown in Table 3. This indicates that a degree of ring-opening polymerization is considered to be roughly controlled by surface area of nanoparticle. The larger PG/core weight ratio in SPION-PG implies the better aqueous solubility of SPION-PG than that of ND-PG, as will be discussed below.

2.3. Chromatographic Separation of Highly Soluble SPION-PG

SPION-PG was soluble in pure water, PBS, and a phosphate buffer (20 mM, pH 7.0) containing Na_2SO_4 (100 mM) (a mobile phase for chromatographic separation), and the solubility was found to be more than 40, 25, and 20 mg mL^{-1}, respectively. Since we only used limited amount of the SPION-PG to determine the above solubility, actual solubility is expected to be larger than the above one. Under acidic conditions at a pH value below 4, no precipitation was observed in the SPION-PG solution of 20 mg mL^{-1}, which is in marked contrast with the poly(acrylic acid)-coated SPION (SPION-PAA).[36] While carboxylates in SPION-PAA were converted to carboxylic acids under acidic conditions to facilitate the aggregation through hydrogen bonding, the neutral hydroxyl groups in SPION-PG are not affected by pH value in the media.[23] Such non-ionic and highly hydrophilic characteristics of PG may afford a "stealth" effect similar to PEG to avoid non-specific interaction with opsonin proteins and uptake by the reticuloendothelial system (RES), improving biocompatibility and blood circulation times.[2,3,22,30,37] Owing to the firm binding of SPION–TREG and TREG–PG discussed above, these aqueous solutions of the SPION-PG were very stable without any aggregation; neither precipitation nor significant change in the hydrodynamic diameter was observed for more than eight months. Such high stability of non-aggregated, or individualized, form is also important for biomedical application to avoid reduction of targeting efficiency, uptake by RES, and risk of embolism.[22] Even freeze-dried solid sample can be readily redispersed in water without any insoluble precipitates. SPION-PG exhibits much higher solubility than as-synthesized SPION[26] and most of the

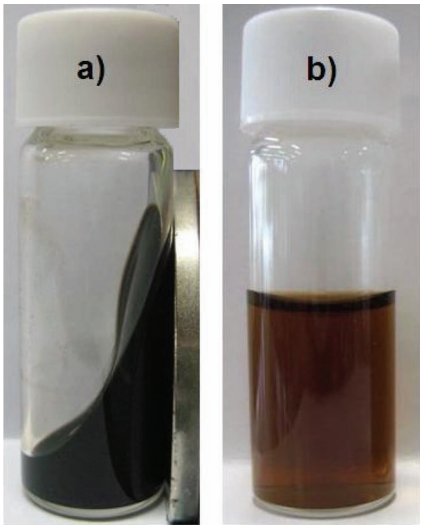

Figure 4. Photographs of a) an aqueous solution of SPION-PG (40 mg/mL) in response to a permanent magnet and b) SPION-PG-RGD dissolved in PBS (1.0 mg/mL).

Table 2. Structural and magnetic properties of SPION-PG before and after chromatographic separation.

Sample	Retention time [min]	Core size[a)] [nm]	Surface area[b)] [nm^2]	Hydrodynamic size[c)] [nm]	Size difference[d)] [nm]	Thickness of PG[e)] [nm]	r_2 [mM^{-1} s^{-1}]
before separation	–	8.8 ± 2.3	243	24.1 ± 4.4, 24.9 ± 5.1[f)]	16.3 ± 3.8, 17.8 ± 4.6 [f)]	8.2 ± 1.9, 8.9 ± 2.3[f)]	86.30
fraction 1	21.0-24.0	10.2 ± 2.7	327	28.9 ± 5.8	18.7 ± 5.1	9.4 ± 2.6	91.97
fraction 2	24.0-26.0	9.1 ± 1.9	260	24.5 ± 4.5	15.4 ± 4.1	7.7 ± 2.0	86.91
fraction 3	26.0-29.0	7.8 ± 1.7	191	19.4 ± 3.8	11.6 ± 3.4	5.8 ± 1.7	77.91

[a)]Average core size of SPION-PG determined by more than 200 particles in the STEM images (Figure 1c–f); [b)] According to the equation of $4\pi r^2$, where r is average radius of the core; [c)]Mean diameter of the number distribution determined by DLS in buffer, unless otherwise noted; [d)] Difference between core and hydrodynamic sizes; [e)] Half of size difference; [f)]In Milli-Q water.

Table 3. Quantitative comparison of SPION-PG and ND-PG in one particle with average size.

	Core size [nm]	Core weight[a)] [ag]	PG weight [ag]	Weight ratio of PG/core	Number of glycerol unit	Surface area of core [nm^2]	Unit number/surface area [nm^{-2}]
SPION-PG	8.8	1.8	2.9	1.6	2.4×10^4	2.4×10^2	100
ND-PG [b)]	30	50	38	0.76	3.1×10^5	2.8×10^3	110

[a)]According to the equation of $4/3\pi dr^3$, where r is average radius of the core, d is the density of nanoparticles; [b)]Ref. [8].

polymer-coated SPIONs. Strong hydrophilicity and superparamagnetism of SPION-PG are simultaneously demonstrated in Figure 4. When an aqueous solution of SPION-PG (40 mg/mL) was subjected to an external magnetic field, the magnetic nanoparticles together with the aqueous medium were attracted to the magnet due to the superparamagnetism of SPION and strong hydrophilicity of PG.

Such high solubility of SPION-PG in an aqueous solution enables chromatographic separation as in the case of ND-PG.[1,8,22,31] A phosphate buffer (pH 7.0, 20 mM) containing Na_2SO_4 (100 mM) was used as mobile phase (flow rate: 1.0 mL min^{-1}), and the elution was monitored with UV light at 254 nm. The typical elution profiles of SPION-PG and free PG are shown in **Figure 5**. The chromatographic peak at 21-29 min corresponds to the elution of SPION-PG. A very weak peak at 35 min is attributed to free PG included in SPION-PG as an impurity, because the retention time is in accordance with that of the authentic free PG.[8] Three fractions were collected at the retention time of 21–24, 24–26, and 26–29 min from the beginning to the end of SPION-PG elution. These fractions were analyzed by DLS to determine the mean hydrodynamic diameters of the number distribution. The mean number diameter of the core was determined by STEM after desalinization through dialysis against Milli-Q water.

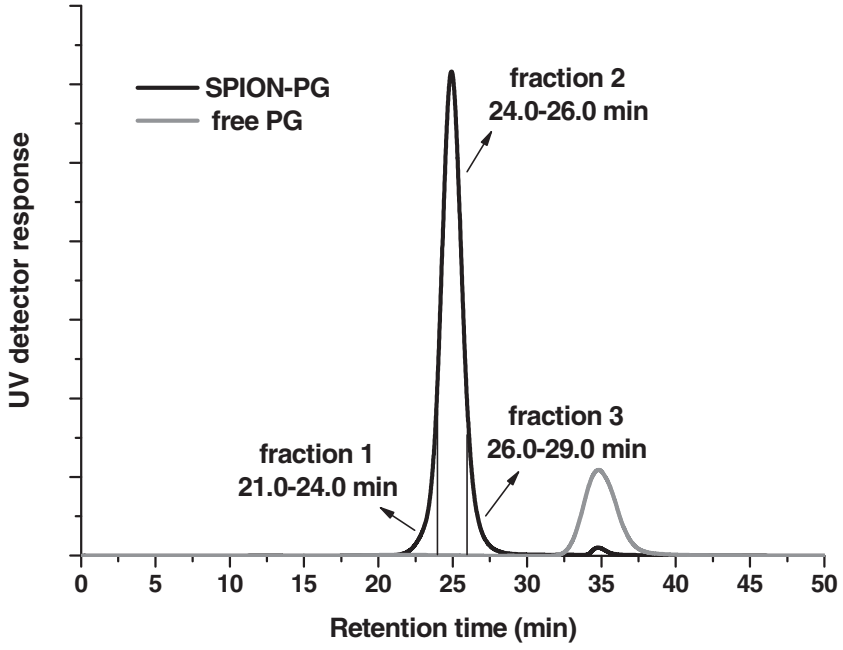

Figure 5. Chromatograms of the elution of SPION-PG and free PG.

The results including SD are summarized in Table 2. As the fraction proceeds from 1 to 3, the core and hydrodynamic diameters as well as the SD decrease from 10.2 ± 2.7 nm to 7.8 ± 1.7 nm (Figure 1d–f) and from 28.9 ± 5.8 nm to 19.4 ± 3.8 nm (Supporting Information Figure S2), respectively. Although fraction 1 has wider size distribution in both core and hydrodynamic sizes than the SPION-PG before separation, the size distributions in fractions 2 and 3 are narrower as suggested by the SD. Post-synthesis SEC offers more precise way to control the particle size. The similar and relatively small SDs in the hydrodynamic size of SPION-PG before and after separation (Table 2) may prove high monodispersibility of SPION-PG. The size difference calculated from the core and hydrodynamic diameters is corresponding to the thickness of the PG layer (Table 2). The thickness and its SD also decrease as the core size decreases in fraction 1–3. Interestingly, the SDs of the core sizes in fractions 1–3 are almost the same as those of the thickness of PG layer, indicating that the core size and thickness of SPION-PG include similar degree of the distribution.

The hydrodynamic size (nm) of the SPION-PG and the thickness (nm) of the PG layer in Table 2 are plotted against the core size (nm) as shown in **Figure 6**. They linearly correlated very well with more than 99.9% correlation coefficient. The following two equations are drawn from these plots in Figure 6:

$$d_{\text{hydrodynamic}} = 4.0 d_{\text{core}} - 11.5 \quad (1)$$

$$t_{\text{PG}} = 1.5 d_{\text{core}} - 5.9 \quad (2)$$

where $d_{\text{hydrodynamic}}$, d_{core}, and t_{PG} are the hydrodynamic and core sizes (nm) of the SPION-PG, and the thickness (nm) of the PG layer, respectively. Since all the SPIONs possess the spherical shape as shown in Figure 1, we can draw the strict linear correlation of hydrodynamic size of the SPION-PG and thickness of PG layer with the core size of the nanoparticle shown in Figure 6 and the above equations. This is not the case of ND-PG because of the inhomogeneous shape of ND.[8] These equations indicate quantitatively that smaller core diameter of SPION-PG leads to smaller hydrodynamic diameter of SPION-PG and thinner PG layer under the same reaction conditions of the PG functionalization. As shown in Table 3, about 100 units of glycerol should exist in unit area (1.0 nm^2) on the surface of the core. Although 100 units of glycerol occupy similar volume on the unit area of the SPION with smaller and larger sizes, smaller size can accommodate

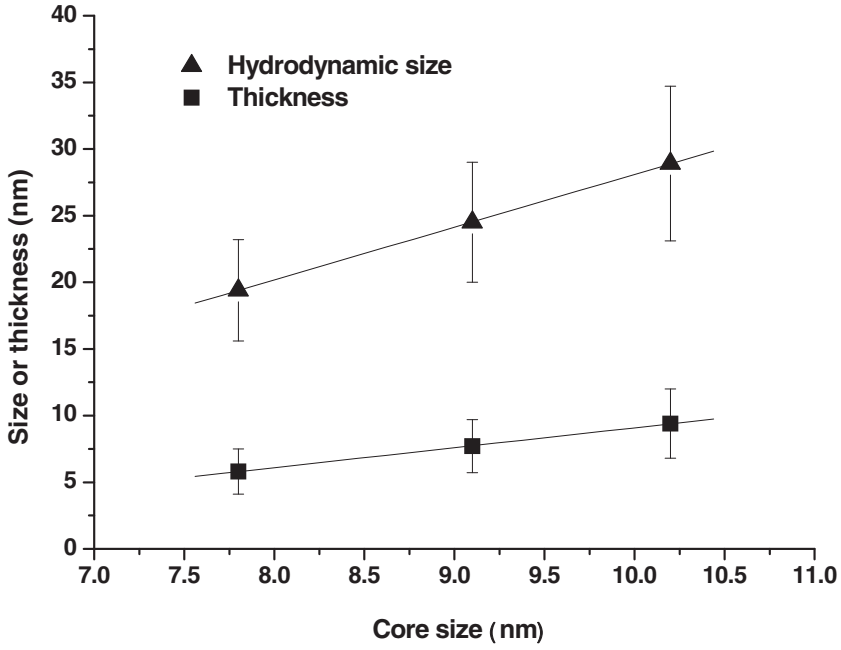

Figure 6. Plots of hydrodynamic size of SPION-PG and thickness of PG layer against the core size. Error bars correspond to standard deviation (SD). Actual values are shown in Table 2.

the same units of glycerol in a thinner space on the surface than larger size because of the larger curvature. This may be the reason why the thickness of the PG layer linearly correlates with the core size of the SPION as shown in Figure 6 and the Equation (2). We hope that these equations are applicable to wider size range and more kinds of spherical nanoparticles functionalized with PG.

2.4. Size Dependence of MRI Relaxivity in SPION-PG

It has been reported that not only the size of SPION but also the thickness of the surface coating affects the magnetic properties of hydrophilic SPIONs.[13,32,33,38,39] As mentioned above, we separated SPION-PG by SEC and defined the core size and the thickness of PG layer as summarized in Table 2. In order to correlate the size parameters of the SPION-PG with the magnetic properties, MRI transverse relaxivity (r_2) were determined by the slope of the linear approximation based on the following equation (Supporting Information Figure S3):

$$1/T_2 = 1/T_2^0 + r_2[\mathrm{Fe}] \quad (3)$$

where T_2 and T^0_2 are the observed transverse relaxation times of SPION-PG and pure water, respectively, and [Fe] is the iron concentration of the solutions. The r_2 of as-synthesized SPION-PG is found to be 86.30 Fe mM^{-1} s^{-1} as shown in Table 2, which is similar to that of the SPION prepared in almost the same process (82.68 Fe mM^{-1} s^{-1}).[26] Since the SPION we prepared was not dissolved well in water as in the case of Santamaria et al.,[30] but not in the case of Cai et al.,[26] we were not able to measure MRI of as-synthesized SPION. Since the core size of our SPION-PG (average diameter: 8.8 ± 2.3 nm in Figure 1a and Table 2) is similar to that of the SPION reported by Cai et al. (particle size: 8 ± 1.1 nm),[26] the similar r_2 of the SPION and SPION-PG can be attributed to little or no effect of the hydrophilic PG functionality on the r_2. Although Bao et al. reported large influence of PEG length on the r_2 of the SPION, the r_2 was stable at the length shorter and longer than the critical length of the PEG, where the r_2 was changed dramatically.[32] Therefore, the TREG and PG on the surface of the SPION might have similar influence of long PEGs such as PEG 2000 and 5000 in the report, which exhibited similar r_2. On the basis of the discussion, the r_2 decrease from fraction 1 to 3 shown in Table 1 can be ascribed to size decrease of the core in SPION-PG, because the large magnetic particles possess higher magnetic moments and hence distort the magnetic field more efficiently to enhance r_2.[23,34,39] Size effect of SPION on r_2 can be concluded to exceed the effect of the PG coating in the case of SPION-PG, at least, in this range of the particle size.

2.5. Further Functionalization of SPION-PG and the Targeting Effect of SPION-PG-RGD

The PG on the surface of SPION not only enhances hydrophilicity to provide SPION with high aqueous solubility and stability as described above, but also offers extensibility to further functionalization to add more functions and properties to SPION-PG. Therefore, we immobilized targeting functionality at the hydroxyl groups in the PG layer through stepwise organic transformation shown in **Scheme 2** and applied it to cells to confirm the targeting efficiency of the further functionalized SPION-PG.[31]

In order to introduce cyclic RGD peptide to target the $\alpha_v\beta_3$-integrin expressed in some kinds of cancer cell, the hydroxyl groups (–OH) in the SPION-PG were converted to tosylate (SPION-PG-OTs), which is a good leaving group frequently used in organic synthesis, and subsequently to azide (SPION-PG-N_3) through nucleophilic substitution of the tosylate with sodium azide.[40] The SPION-PG-N_3 was reacted with cyclic RGD peptide having acetylene terminus through click chemistry,[16,23,41,42] giving SPION-PG-RGD (Scheme 2). These organic transformations were confirmed qualitatively by FTIR as shown in Figure 2 and quantitatively by elemental analysis as shown in Table 1.

The absorption bands at 1600, 1350, and 1176 cm^{-1} in the spectrum of SPION-PG-OTs (Figure 2d) are attributed to the vibrational modes of the benzene ring, asymmetric and symmetric stretchings of S=O bonds, respectively. SPION-PG-N_3 clearly shows characteristic absorption band of azide at 2100 cm^{-1} (Figure 2e). After the click reaction, the azide absorption band was consumed thoroughly to give two new bands at 1660 and 1540 cm^{-1} attributed to C=O and N–H stretchings of amide bonds in cyclic RGD peptides (Figure 2f).

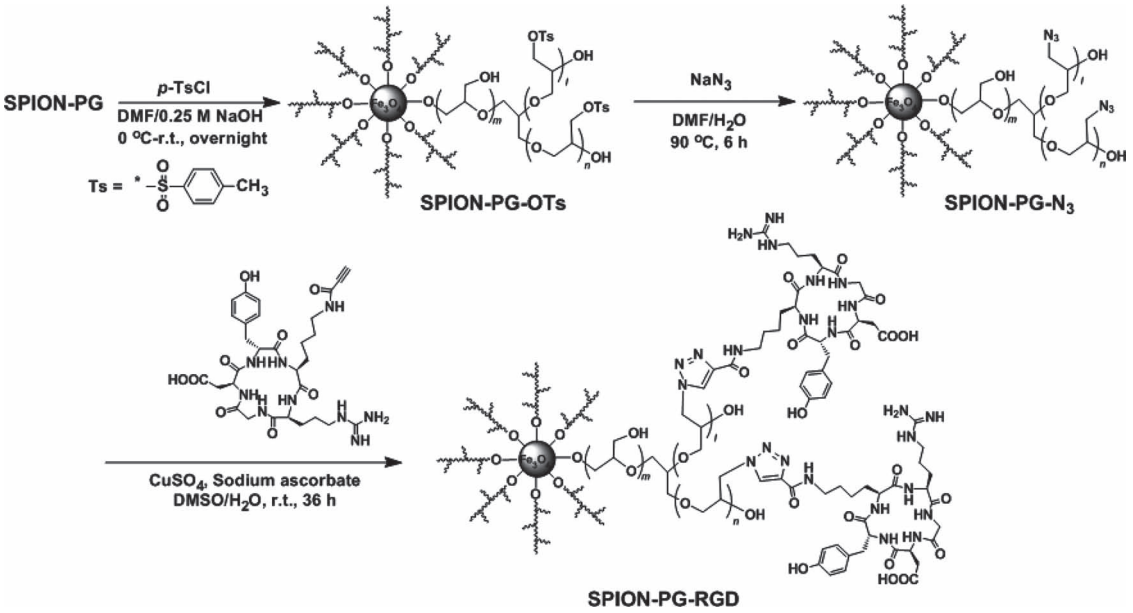

Scheme 2. Synthesis of SPION-PG-RGD from SPION-PG through multistep organic transformations.

The elemental analysis of SPION-PG-N_3 demonstrates the azide functionalization of SPION-PG by appearance of N content and decrease in C and H contents as compared with those of SPION-PG (Table 1). The number of azide in one SPION-PG-N_3 particle and the ratio in numbers of azide and hydroxyl group are calculated from the result of the elemental analysis. As discussed above, the weight of one SPION-PG particle is 4.9 ag and, therefore, the weight of C is 1.5 ag due to the C (wt%) of 30.60%. The number of C atom in one SPION-PG is calculated to be 7.6×10^4, and the same number of C atom should be included in SPION-PG-N_3. Based on the weight% of C and N (24.51% and 1.11%, respectively) in Table 1, the number of azide in one particle is determined to be 9.8×10^2. Since 2.4×10^4 units of glycerol are considered to consist of the PG layer as discussed above, one hydroxyl group out of 24 is converted to azide, which is considered to lead subsequently to RGD quantitatively because of disappearance of absorption of azide in FTIR shown in Figure 2f.

The resulting SPION-PG-RGD exhibited good solubility and stability in PBS as shown in Figure 4b and was applied to cell experiment to confirm the $\alpha_v\beta_3$-integrin targeted cell labeling. SPION-PG and SPION-PG-RGD were incubated with following three kinds of cancer cells; HeLa, U87MG, and A549. The uptake of the nanoparticles was confirmed histologically by Prussian blue staining.[21] No noticeable color change is observed in the cells treated with SPION-PG (upper pictures in **Figure 7**), indicating that SPION-PG cannot internalize into the cells through the cell membrane. In contrast, U87MG and A549 treated by SPION-PG-RGD were stained blue, while HeLa was not stained (lower pictures in Figure 7). Since cyclic RGD peptide is known to have affinity to $\alpha_v\beta_3$-integrin,[43,44] a degree of blue staining may depend on number of the integrin expressed in the cells. U87MG and A549 are well-known to overexpress the integrin,[45,46] facilitating the internalization of SPION-PG-RGD into the cells. On the other hand, HeLa is concluded to have much less number of the integrin than U87MG and A549.[47] In the stained cells shown in Figure 7, sporadic blue spots were detected in the perinuclear cytoplasmic vesicles of U87MG and A549 cells.[45,46] These results suggest that SPION-PG-RGD was incorporated into the cells through receptor-mediated endocytosis based on the affinity of cyclic RGD peptide to the integrin.[43,44,47] The targeting efficacy of SPION-PG-RGD demonstrated here together with high solubility and MRI relaxivities of SPION-PG described above indicate that SPIO-PG-RGD possesses a great potential as an agent for in vivo cancer imaging and therapy.

3. Conclusions

A PG coating provided SPION with excellent solubility and stability in a physiological medium as well as good extensibility to add more functions such as targeting effect. Because PG is also reported to be biocompatible[9] and resistant to protein adsorption,[10] PG is considered as one of the ideal surface functionality for nanoparticle in view of biomedical application. We demonstrated direct PG grafting of SPION prepared by polyol method and characterization of SPION and SPION-PG qualitatively using FTIR, STEM, and DLS, and quantitatively using elemental analysis and TGA. From the quantitative discussion, various structural characteristics of SPION-PG were disclosed such as the weights of the inner core and the outer shell, and number of glycerol unit consisting of the PG layer. Since SPION-PG exhibited high solubility even in a buffer solution, SPION-PG was separated according to the size by chromatography. The hydrodynamic size of SPION-PG and the thickness of PG were found to correlate linearly with the core size, indicating that the core size controls the thickness of the coating. The core size also affected the magnetic properties of SPION-PG, but the thickness of the PG layer was considered to cause

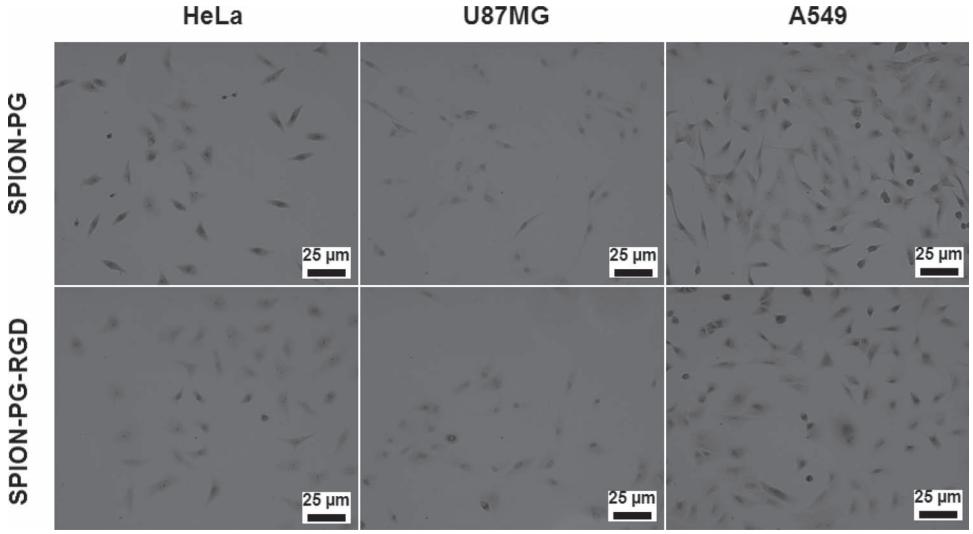

Figure 7. Prussian blue stained images of cancer cells treated with SPION-PG (upper) and SPION-PG-RGD (lower).

less influence. In view of biomedical applications, the targeting moiety was immobilized by utilizing good extensibility of PG; the hydroxyl groups in PG was converted to azide through multistep organic transformations, and RGD peptide was conjugated covalently through click chemistry. The resulting SPION-PG-RGD demonstrated targeting specificity towards cancer cells overexpressing $\alpha_v\beta_3$-integrin such as A549 and U87MG cancer cells. We believe that SPION-PG with targeting functionality works as an imaging probe, a drug carrier, and a hyperthermic agent in vivo, and makes a breakthrough in the field of nanomedicine.

4. Experimental Section

Chemicals: Chemicals were used as received, unless otherwise noted. Iron (III) acetylacetonate ($Fe(acac)_3$), *N*-hydroxysuccinimide (NHS), and *N*,*N*-dicyclohexyl carbodiimide (DCC) were obtained from Nacalai Tesque Inc. $Fe(acac)_3$ was purified by recrystallization from water/methanol before use. Glycidol purchased from Kanto Chemical Co., Ltd was dried over 4 Å molecular sieves prior to use. Propiolic acid was purchased from TCI. cyclic RGD (Arg-Gly-Asp-D-Tyr-Lys) was purchased from Peptides International, Inc. The mobile phase of the SEC was prepared by diluting the commercial pH 7.0 phosphate buffer (100 mM, Nacalai Tesque Inc.) five times followed by adding solid Na_2SO_4 to make the concentration in the phosphate buffer to be 100 mM.

Synthesis of Succinimidyl-3-propiolate: This compound was synthesized according to the reported procedure with minor modification.[48] DCC (0.169 g, 3.0 mmol) in ethyl acetate (10 mL) was added dropwise to a solution of propiolic acid (0.21 g, 3.0 mmol) and NHS (0.345 g, 3.0 mmol) in ethyl acetate (20 mL) in ice/water bath with vigorous stirring. The reaction was kept at 4 °C for 4 h, and then warmed up to room temperature and stirred overnight. After filtration, the filtrate was concentrated to give yellow solid. The crude product was purified by recrystallization from dichloromethane/hexane and dried in vacuo, giving light yellow crystalline (0.36 g, 2.2 mmol) in 72% yield. mp: 89–91 °C, ^{1}H NMR (270 MHz, $CDCl_3$, δ) 3.31 (s, 1H), 2.88 (s, 4H).

Synthesis of RGD Propargyl Amide: Cyclic RGD peptide (10.0 mg, 16.2 μmol) and succinimidyl-3-propiolate (2.7mg, 16.2 μmol) were dissolved in DMSO (1.0 mL) and stirred at room temperature for 48 h. After evaporation of DMSO, the residue were dispersed in water and filtered to remove insoluble impurities. The desired product was obtained with a retention time of 15.4 min on an analytical HPLC, and used without further purification. ESI-MS: *m*/*z* 672.40 for $[M+H]^+$ ($C_{30}H_{41}N_9O_9$, calculated molecular weight: 671.30) (Supporting Information Figure S4).

Preparation of SPION-PG: SPION was prepared according to the published polyol method with slight modification.[26] Briefly, $Fe(acac)_3$ (0.53 g, 1.5 mmol) and triethylene glycol (30 mL) were mixed with the aid of bath sonication, then slowly heated to reflux over 3 h under an argon atmosphere. After cooling down, ethyl acetate (20 mL) was added to the blackish homogeneous suspension, which mixed by magnetic stirring. The nanoparticles were collected by centrifugation (50 400 *g*, 20 min) and washed with ethyl acetate for 4 times, then dried in vacuo to give a blackish solid (0.13 g). After a suspension of thus synthesized SPION (30 mg) in glycidol (6.0 mL) was sonicated at 25 °C for 1 h, the resulting dispersion was magnetically stirred at 140 °C under an argon atmosphere for 20 h and then allowed to cool down to room temperature. The resulting blackish gel was diluted with Milli-Q water (20 mL) in an ultrasonic bath, and the precipitates were recovered after ultracentrifugation at 543 200 *g* for 20 min. This washing process was repeated four times to remove free PG. The washed sample was lyophilized to give a blackish flocculent solid (52.3 mg).

The core sizes of the SPION before and after PG functionalization were determined with STEM by measuring the sizes of more than 200 particles using Nano Measurer 1.2.5 (Jie Xu, Fudan University). The mean hydrodynamic diameters of the number distribution in aqueous solutions of the SPION-PG (Table 2) were determined by DLS on a Nanotrac UPA-UT151 (Microtrac, Inc.).

Solubility of SPION-PG was determined as follows; an aliquot (100 μL) of a solution of SPION-PG in Milli-Q water was dropped into a tin boat (4 × 4 × 11 mm, Elementar Analysensysteme GmbH), thoroughly dried at 60 °C overnight, and weighed the dried solid with a microbalance (XP-6, Mettler-Toledo International Inc.). The procedure was repeated three times and the average value was used as the solubility. Solubility of a buffer solution of SPION-PG was determined in a similar way, after it was dialyzed against Milli-Q water (Spectra/Pro dialysis membrane, MWCO: 12–14 kDa).

Synthesis of SPION-PG-OTs: SPION-PG (30 mg) was dissolved in an aqueous solution of NaOH (0.25 M, 6.0 mL) by bath sonication and then cooled down to 0 °C in an ice bath. *p*-Toluenesulfonyl chloride (30 mg, 0.16 mmol) was dissolved in DMF (6.0 mL) and added dropwise into the mixture under rapid stirring. The solution was stirred at 0-5 °C for 3 h and at room temperature for 10 h. The resulting solid was collected by ultracentrifugation and purified in DMF/water by repeated redispersion/ultracentrifugation cycles.

Synthesis of SPION-PG-N_3: Sodium azide (20 mg, 0.31 mmol) in water (2.0 mL) was added into SPION-PG-OTs (20 mg) in DMF (6.0 mL) and stirred at 90 °C for 6 h under an argon atmosphere. After cooling down, the product was collected by ultracentrifuge and purified in water by repeated redispersion/ultracentrifugation cycles.

Synthesis of SPION-PG-RGD: RGD propargyl amide (2.0 mg) in DMSO (1.0 mL) was added to a solution of SPION-PG-N_3 (12 mg) in water (1.5 mL). Copper(II) sulfate pentahydrate (5.8 mg) in water (0.5 mL) and sodium ascorbate (8.4 mg) in water (0.5 mL) were added into the mixture with vigorous stirring. The resulting brown suspension was bath sonicated for 5 min and stirred at room temperature for 36 h. Diluted ammonia was dropped into the suspension to dissolve insoluble copper salts, giving a clear brown solution. The solid was collected by ultracentrifugation and purified in 1% ammonia by repeated washing/ultracentrifugation. The purified sample was dialyzed against PBS to replace the medium to a physiological solution for cell experiments.

Size Sorting of SPION-PG by SEC: Chromatographic size separation of SPION-PG was conducted according to the procedures described previously.[8] The following three columns were connected for SEC separation of SPION-PG: Cosmosil CNT-2000, CNT-1000, and CNT-300 (diameter: 7.5 mm, length: 300 mm, Nacalai Tesque Inc.) with pore sizes of 2000, 1000, and 300 Å, respectively. A phosphate buffer (20 mm, pH 7.0) containing Na_2SO_4 (100 mm) was used as the mobile phase with a flow rate of 1.0 mL min^{-1}. After the injection of the solution of SPION-PG in the buffer (5.0 mg mL^{-1}, 2.5 mL), elution was monitored with UV light at 254 nm. Three fractions with 21–24, 24–26 and 26–29 min in retention time were collected. The number-based mean hydrodynamic diameters in these solutions (Table 2) were determined by DLS on a Nanotrac UPA-UT151 (Microtrac, Inc.).

Measuring MRI Relaxivity of SPION-PG: Samples were desalinized and then well dispersed in Milli-Q water with known Fe concentration (determined by ICP-OES). Short NMR tubes containing diluted samples with varying Fe concentration were fixed in a water bath at room temperature. The magnetometric measurements were conducted on a MRI system (Agilent, UNITY INOVA) with a 7-Tesla magnet (JASTEC) and a magnetic field gradient coil (Magnex). MR images were obtained by a spin echo sequence (reception time (TR) = 4000 ms, echo time (TE) = 14, 18, 50, 80, 100, 120 ms, slice thickness = 2 mm, and field of view = 40 × 40 mm^2). Region-of-interest (ROI) was set on the tubes and the signal intensities were measured for each concentration. The T_2 values were calculated by exponential fitting.

Cellular Labeling: The cells (8×10^3 cells per well in 4-well LabTek chamber slides [BD bioscience]) cultured in Dulbecco's modified Eagle's medium (DMEM) containing 10% fetal bovine serum were incubated for 72 h with 140 μg/ml of SPION-PG or SPION-PG-RGD. After incubation, the culture medium was removed and the adherent cells were washed thrice with 1× PBS, and fixed with 1% buffered formaldehyde and 70% ethanol. For Prussian blue staining, the fixed cells were washed thrice with 1 × PBS, incubated with 1% potassium ferrocyanide in 0.5% hydrochloric acid for 20 min, and counterstained with nuclear fast red.

Supporting Information

Supporting Information is available from the Wiley Online Library or from the author.

Acknowledgements

This work was supported financially by Science and Technology Incubation Program in Advanced Region (JST), Industrial Technology Research Grant Program (NEDO), and Grant-in-Aid for Challenging Exploratory Research (JSPS).

Received: April 17, 2012
Revised: June 23, 2012
Published online: August 7, 2012

[1] U. I. Tromsdorf, O. T. Bruns, S. C. Salmen, U. Beisiegel, H. Weller, *Nano Lett.* **2009**, *9*, 4434.
[2] H. Lee, E. Lee, D. K. Kim, N. K. Jang, Y. Y. Jeong, S. Jon, *J. Am. Chem. Soc.* **2006**, *128*, 7383.
[3] A. S. Karakoti, S. Das, S. Thevuthasan, S. Seal, *Angew. Chem. Int. Ed.* **2011**, *50*, 1980
[4] T. Takimoto, T. Chano, S. Shimizu, H. Okabe, M. Ito, M. Morita, T. Kimura, T. Inubushi, N. Komatsu, *Chem. Mater.* **2010**, *22*, 3462.
[5] M. Calderón, M. A. Quadir, S. K. Sharma, R. Haag, *Adv. Mater.* **2010**, *22*, 190.
[6] D. Wilms, S.-E. Stiriba, H. Frey, *Acc. Chem. Res.* **2010**, *43*, 129.
[7] L. Wang, K. G. Neoh, E. T. Kang, B. Shuter, S.-C. Wang, *Adv. Funct. Mater.* **2009**, *19*, 2615.
[8] L. Zhao, T. Takimoto, M. Ito, N. Kitagawa, T. Kimura, N. Komatsu, *Angew. Chem. Int. Ed.* **2011**, *50*, 1388.
[9] A. L. Sisson, D. Steinhilber, T. Rossow, P. Welker, K. Licha, R. Haag, *Angew. Chem. Int. Ed.* **2009**, *48*, 7540.
[10] P.-Y. J. Yeh, R. K. Kainthan, Y. Zou, M. Chiao, J. N. Kizhakkedathu, *Langmuir* **2008**, *24*, 4907.
[11] L. Zhao, T. Takimoto, T. Kimura, N. Komatsu, *J. Indian Chem. Soc.* **2011**, *88*, 1787.
[12] W. J. Stark, *Angew. Chem. Int. Ed.* **2011**, *50*, 1242.
[13] E. Amstad, M. Textor, E. Reimhult, *Nanoscale* **2011**, *3*, 2819.
[14] J. Xie, G. Liu, H. S. Eden, H. Al, X. Chen, *Acc. Chem. Res.* **2011**, *44*, 883.
[15] R. Hao, R. Xing, Z. Xu, Y. Hou, S. Gao, S. Sun, *Adv. Mater.* **2010**, *22*, 2729.
[16] A. H. Latham, M. E. Williems, *Acc. Chem. Res.* **2008**, *41*, 411.
[17] S. Laurent, D. Forge, M. Port, A. Roch, C. Robic, L. V. Elst, R. N. Muller, *Chem. Rev.* **2008**, *108*, 2064.
[18] Y. Jun, J.-H. Lee, J. Cheon, *Angew. Chem. Int. Ed.* **2008**, *47*, 5122.
[19] A. K. Gupta, M. Gupta, *Biomaterials* **2005**, *26*, 3995.
[20] M. Colombo, S. Carregal-Romero, M. F. Casula, L. Gutierrez, M. P. Morales, I. B. Bohm, J. T. Heverhagen, D. Prosperi, W. J. Parak, *Chem. Soc. Rev.* **2012**, *41*, 4306.
[21] K. Chen, J. Xie, H. Xu, D. Behera, M. H. Michalski, S. Biswal, A. Wang, X. Chen, *Biomaterials* **2009**, *30*, 6912.
[22] F. M. Kievit, Z. R. Stephen, O. Veiseh, H. Arami, T. Wang, V. P. Lai, J. O. Park, R. G. Ellenbogen, M. L. Disis, M. Zhang, *ACS Nano* **2012**, *6*, 2591.
[23] H. B. Na, G. Palui, J. T. Rosenberg, X. Ji, S. C. Grant, H. Mattoussi, *ACS Nano* **2012**, *6*, 389.
[24] E. Amstad, T. Gillich, I. Bilecka, M. Textor, E. Reimhult, *Nano Lett.* **2009**, *9*, 4042.
[25] W. Cai, J. Wan, *J. Colloid Interface Sci.* **2007**, *305*, 366.
[26] J. Wan, W. Cai, X. Meng, E. Liu, *Chem. Commun.* **2007**, 5004.
[27] F. Alexis, E. Pridgen, L. K. Molnar, O. C. Farokhzad, *Mol. Pharm.* **2008**, *5*, 505.
[28] S. Cheong, P. Ferguson, K. W. Feindel, I. F. Hermans, P. T. Callaghan, C. Meyer, A. Slocombe, C.-H. Su, F.-Y. Cheng, C.-S. Yeh, B. Ingham, M. F. Toney, R. D. Tilley, *Angew. Chem. Int. Ed.* **2011**, *50*, 4206.
[29] A.-H. Lu, E. L. Salabas, F. Schuth, *Angew. Chem. Int. Ed.* **2007**, *46*, 1222.
[30] N. Miguel-Sancho, O. Bomati-Miguel, G. Colom, J.-P. Salvador, M.-P. Marco, J. Santamaria, *Chem. Mater.* **2011**, *23*, 2795.
[31] H. Wei, N. Insin, J. Y. Lee, H.-S. Han, J. M. Cordero, W. Liu, M. G. Bawendi, *Nano Lett.* **2012**, *12*, 22.
[32] S. Tong, S. Hou, Z. Zheng, J. Zhou, G. Bao, *Nano Lett.* **2010**, *10*, 4607.
[33] H. Duan, M. Kuang, X. Wang, Y. A. Wang, H. Mao, S. Nie, *J. Phys. Chem. C* **2008**, *112*, 8127.
[34] Y. Jun, Y.-M. Huh, J. Choi, J.-H. Lee, H.-T. Song, S. Kim, S. Yoon, K.-S. Kim, J.-S. Shin, J.-S. Suh, J. Cheon, *J. Am. Chem. Soc.* **2005**, *127*, 5732.
[35] D. Maity, S. N. Kale, R. Kaul-Ghanekar, J.-M. Xue, J. Ding, *J. Magn. Magn. Mater.* **2009**, *321*, 3093.

[36] J. Ge, Y. Hu, M. Biasini, C. Dong, J. Guo, W. P. Beyermann, Y. Yin, *Chem. Eur. J.* **2007**, *13*, 7153.
[37] J. A. Barreto, W. O'Malley, M. Kubeil, B. Graham, H. Stephan, L. Spiccia, *Adv. Heathcare Mater.* **2011**, *23*, H18.
[38] L. E. W. LaConte, N. Nitin, O. Zurkiya, D. Caruntu, C. J. O'Connor, X. Hu, G. Bao, *J. Magn. Reson. Imaging* **2007**, *26*, 1634.
[39] J. Huang, L. Bu, J. Xie, K. Chen, Z. Cheng, X. Li, X. Chen, *ACS Nano* **2010**, *4*, 7151.
[40] W.-W. Zheng, Y.-H. Hsieh, Y.-C. Chiu, S.-J. Cai, C.-L. Cheng, C. Chen, *J. Mater. Chem.* **2009**, *19*, 8432.
[41] M. A. White, J. A. Johnson, J. T. Koberstein, N. J. Turro, *J. Am. Chem. Soc.* **2006**, *128*, 11356.
[42] T. Meinhardt, D. Lang, H. Dill, A. Krueger, *Adv. Funct. Mater.* **2011**, *21*, 494.
[43] P. Decuzzi, M. Ferrari, *Biomaterials* **2007**, *28*, 2915.
[44] J.-P. Xiong, T. Stehle, R. Zhang, A. Joachimiak, M. Frech, S. L. Goodman, M. A. Arnaout, *Science* **2002**, *296*, 151.
[45] W. Cai, X. Chen, *Nat. Protoc.* **2008**, *3*, 89.
[46] S. Meng, B. Su, W. Li, Y. Ding, L. Tang, W. Zhou, Y. Song, Z. Caicun, *Med. Oncol.* **2011**, *28*, 1180.
[47] Q. Xu, Y. Liu, S. Su, W. Li, C. Chen, Y. Wu, *Biomaterials* **2012**, *33*, 1627.
[48] J. Chao, W.-Y. Huang, J. Wang, S.-J. Xiao, Y.-C. Tang, J.-N. Liu, *Biomacromolecules* **2009**, *10*, 877.